NiO modified Biochar for efficient adsorption of cationic dye

Layla El Moussaoui[1*], *Majda* Ben Ali[2], *Abdellah* Benzaouak[3], *Yassine* Elkahoui[2], *Oumaima* Sadik[1], *Mouatamid* El hazzat[1], *Abdelkebir* Bellaouchou[1] *and Adnane* El Hamidi[1]

[1] Laboratory of Materials, Nanotechnologies and Environment, Faculty of Sciences, Mohammed V University in Rabat, Morocco

[2] Laboratory of Spectroscopy, Molecular Modeling, Materials, Nanomaterials, Water and Environment (LS3MN2E), Department of Chemistry, Faculty of Sciences, Mohammed V University in Rabat, Morocco

[3] Laboratory of Spectroscopy, Molecular Modeling, Materials, Nanomaterials, Water and Environment, Environmental Materials Team, ENSAM, Mohammed V University in Rabat, Morocco

Abstract. There is a rising production of urban sewage sludge (SS) and the continuous discharge of methylene blue dye (MB) effluent from textile and pharmaceutical industries are posing a serious environmental challenge. In this study, SS was valorized using a thermal and chemical treatment to improve its absorption capacity to adsorb MB in contaminated aqueous solutions. The adsorbent prepared (NiO-BCHCl) was further evaluated for the removal of MB dye. Several experimental techniques were used to characterize the material and related adsorption mechanisms. According to BET measurements, the specific surface area was found to be 48.32 m²/g was identified, and SEM/EDS confirmed a good incorporation of oxide on the biochar surface. The adsorption process follows the Sips isotherm model and the second-order kinetic model. This study suggests that a composite of NiO and SS Biochar provides a high-performance and low-cost material for water treatment.

Keywords: sewage sludge; nickel oxide; wastewater; methylene blue; biochar; adsorption; dye.

1. Introduction

Water pollution is one of the most critical environmental issues globally, menacing both the environment and human health. Rapid industrial growth, population rise, and urbanization have resulted in the release of significant amounts of untreated treated wastewater into aquatic ecosystems [1]. Besides destroying aquatic systems, water contamination reduces the amount of clean water available for industrial, agricultural, and residential uses. Prolonged exposure to tainted water has been linked to major health complications [2, 3, 4, 5].

Given to their wide use and environmental longevity, synthetic dyes are one of the most concerning types of pollutants. Methylene blue (MB), as a cationic dye, is extensively include textiles, paper, leather, plastics, and medicine [6, 7]. When released, MB and other dyes can obscure light in aquatic environments, which interferes with photosynthesis [8]. MB is also difficult to eliminate naturally, and it is visible even in trace concentrations. Furthermore, exposure to MB can have harmful effects on human beings, including nausea, eye irritation, and in some cases, poisonous and mutagenic effects [9, 10].

Researchers are looking for sustainable and inexpensive adsorbents to deal with dye contamination in water. The valorization of urban sewage sludge (SS), an outcome of wastewater treatment plants, is one of water decontamination solutions [11]. SS which is usually looked at as a problematic waste because of its large volume and environmental hazards, can be transformed, by thermal process under limited oxygen, into porous biochar with adsorptive properties, leading to a performant adsorbent that can eliminate a variety of pollutants from water and reducing trash at the same time [12, 13]. To improve of biochar surface, a post-treatment using chloric acid can be useful to enhance porosity and surface area. Furthermore, incorporation of metals or metallic oxides on the biochar can significantly enhance its adsorption efficiency. NiO is known for its redox properties and strong affinity toward cationic pollutants such as methylene blue [14, 15, 16]. In this study, we focus on preparing a composite af nickel oxide and biochar washed with HCl. The synthesized composite was evaluated for its capacity to adsorb methylene blue from aqueous solutions. The effects of relevant variables were studied and adsorption mechanisms were investigated through kinetic and equilibrium modeling.

* Corresponding authors: Layla_elmoussaoui@um5.ac.ma

2. Materiels and methods

2.1. Materials

Oxide-biochar nanocomposite was prepared using Municipal sludge collected in domestic a Moroccan wastewater treatment plant.
The pollutant used to study the adsorptive performance of the prepared sample was Methylene blue as a cationic dye.
Several stages were included in the experimental procedure. Firstly, drying of the SS was performed in an oven at 120°C for 2 nights then ground. The obtained powder was carbonized for 1h in a limited oxygen atmosphere the temperature was increased to 550°C at a rate of 10°C/min in a programmable furnace.
The carbonized biochar was immersed in an HCl solution of 0.5 M for 2H, washed several times until neutralization, then dried to obtain BCHCl.

To prepare the composite of oxide and Biochar, 1 g of biochar was mixed in a nickel chloride solution of a predetermined concentration. NaOH solution was added drop by drop and then the mixture was kept under continuous magnetic stirring for 2 hours. The obtained precipitate was then filtered, washed five times with distilled water, dried overnight, and finally calcined at 500°C to obtain the adsorbent sample NiO-BCHCl.

2.2. Characterizations of the prepared sample

SEM (Scanning Electron Microscopy) with EDS (Energy Dispersive Spectroscopy) was used to study the Surface morphology and the elemental composition of synthesized products.
Nitrogen adsorption measurements were carried out determined at 77 K using a NOVA 2200 analyzer from Quantachrome Corp. To determine the specific surface area (SBET) of the samples, based using the Brunauer–Emmett–Teller (BET) approach.

2.3. Methods

2.3.1 Modeling Adsorption Kinetics and Equilibrium Behavior

The kinetics of adsorption were investigated using the Lagergren pseudo-first-order and pseudo-second-order kinetic models (Eqs. 1 and 2) [17, 18]. For the characterization of adsorption equilibria the Langmuir (Eq. 3) [19], Freundlich (Eq. 4), and Sips (Eq. 5) adsorption isotherm models were fit to the experimental data [20, 21]. The mathematical expressions of these models are as presented :

- Analysis using the pseudo-first-order kinetic model

$$Q_t = Q_e(1 - e^{-k_1 t})$$

In this model, Q_e (mg. g^{-1}) refers to the adsorption capacity, and Q_t (mg. g^{-1}) corresponds to the amount of adsorbate taken up at a given time t. The pseudo-first-order kinetic constant, k_1 (min^{-1}), is obtained from the linear regression of ln (Q_e - Q_t) against time.

- Second-order kinetic model

$$Q_t = \frac{k_2 Q_e^2 t}{1 + k_2 Q_e}$$

Here, k_2 ($(g.mg^{-1}.min^{-1})$): kinetic constant

- Langmuir isotherm:

$$Q_e = \frac{Q_m K_L C_e}{1 + C_e K_L}$$

Qe ($mg \cdot g^{-1}$) indicates the adsorbate amount captured at equilibrium, while C_e (mg L^{-1}) is its concentration in solution at equilibrium. Q_m (mg. g^{-1}) defines the maximum adsorption capacity, and K_L (L. mg^{-1}) is Langmuir equilibrium associated with the free energy of adsorption.

- Freundlich isotherm:

$$Q_e = K_f C_e^{\frac{1}{n}}$$

The Freundlich constant, K_f (mg/g) $(mg/L)^{-1/n}$), indicates the adsorption capacity of the material, whereas the empirical parameter 1/n represents the adsorbent's surface affinity for the adsorbate.

- Adsorption isotherm according to Sips :

$$Q_e = \frac{Q_m(K_S C_e)^n}{1+(K_S C_e)^n}$$

In the Sips model, Q_m denotes the maximum adsorption capacity ($mg \cdot g^{-1}$), a_s indicates the strength of adsorption interaction $(L/mg)^n$, and n represents variability of surface sites, reflecting the surface heterogeneity of the adsorbent.

3. Experimental Results and Discussion

3.1. Point of zero charge (pH_{pzc})

Figure 1 depicts the point of zero charge (pHpzc) for the raw sludge, the biochar, and the NiO–Biochar composite. The determination of pHpzc was done by varying the pH of the solution from 2 to 12. The pHpzc of raw sludge was found to be 5.66, suggesting that this pH is where the sludge's surface becomes electrically neutral. The biochar was slightly increased in the pHpzc value to 6.2, which could indicate an increase in the abundance of surface basic functional groups like hydroxyl (–OH) and carboxylate ($–COO^-$) functional groups that favored protonation. The development of NiO–Biochar caused a small decrease in the pHpzc to 4.23, indicating a slight reduction of surface basicity. This was likely due to the interactions of nickel species with the oxygen-containing functional groups of biochar, restricting the availability of these functional groups to undergo proton transfer or deprotonation for protons in solution. The modification of the surfaces changed electrostatic interactions with both positively and negatively charged ions in solution, affecting the adsorption behavior [22].

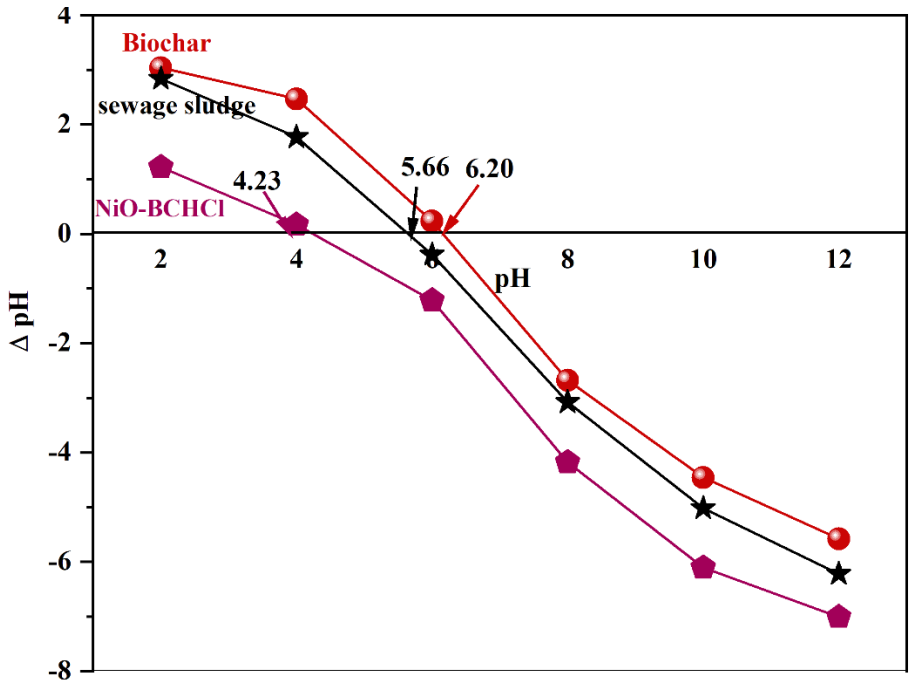

Fig. 1. Zero Charge Point of NiO-BCHCl

3.2. Surface area (BET)

The results presented in Table 1 indicate that SS has a very low specific surface area compared to biochar obtained after pseudo-pyrolysis, which limits interaction capacity. After the thermal and HCl treatment. The subsequent deposition of NiO oxide onto biochar further improved the surface area, due to the fine dispersion of oxide

nanoparticles on the surface, which provides additional surface sites and contributes to additional textural improvements [23, 24].

Table 1. Evolution of Specific Surface Area

Sample	**S_{BET} (m^2/g)**
Dried sewage sludge (SS)	3.39
Sewage sludge-derived Biochar (SSBC)	37.44
NiO-BCHCl	48.32

3.3. SEM/EDS/MAPPING

The SEM image of NiO-BCHCl (Fig. 2) displays a layered texture, corresponding to carbonized biochar structures typical of carbonaceous material after thermal treatment. The bright spots on the biochar surface are likely associated with electron-dense materials, which are NiO oxide. They had a spherical or globular morphology with no significant agglomeration, indicating a relatively homogenous distribution of oxide on the surface and therefore good adsorptive performance. Adhesion between the BC and NiO was clearly demonstrated, with NiO visibly coating the surface of Biochar [25]. The recorded EDS spectra (Fig. 2b) for the prepared sample is shown in fig .2, indicating the presence of Ni, O along with other elements from Biochar like C, Si and Si which confirms the formation of the composite. Additionally, the elemental mapping analysis revealed a uniform distribution of nickel (depicted in yellow) and other elements of biochar as illustrated in Fig. 2c.

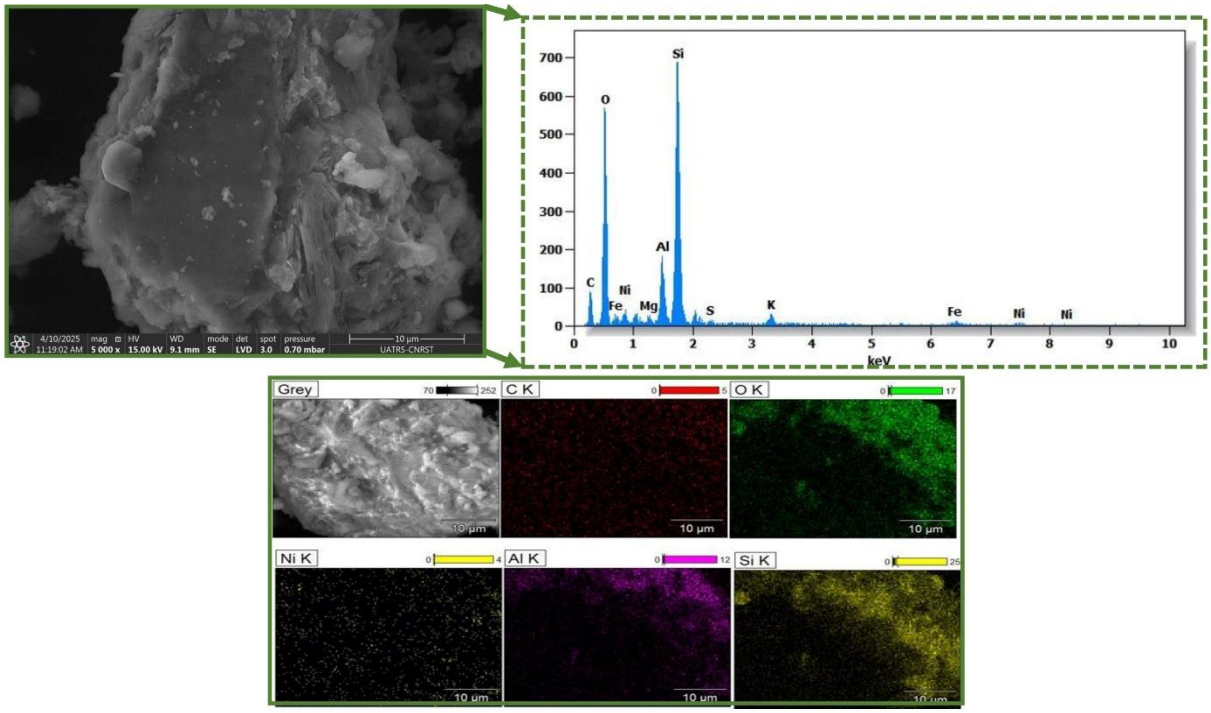

Fig. 2. SEM/EDS Analysis and Elemental Mapping of NiO-BCHCl

3.4. Adsorption experiments

The adsorption performance of methylene blue onto NiO-BCHCl was evaluated by varying the following operational parameters: adsorbent mass, pH, and initial MB concentration.

3.4.1. Mass effect

To evaluate the effectiveness of BM removal by prepared composite (Fig. 3), different adsorbent masses ranging from 0.5 to 2 g/L were investigated. The BM concentration used was 20 ppm, with a contact time of 3.5 hours,

and the pH maintained was that of the MB solution. Fig.4 illustrates the variation of the adsorbent mass as a function of the MB removal rate [26].

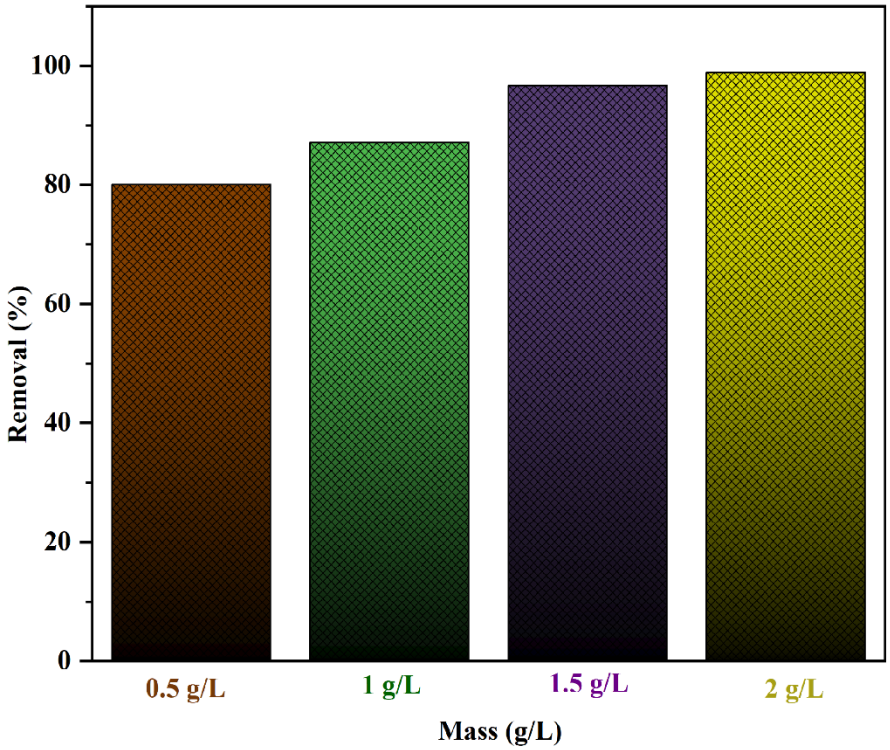

Fig. 3. Effect of NiO-BCHCl Mass on MB Removal

Fig.3. shows that the adsorption of the dye MB gradually increases with an increase in adsorbent mass and achieved nearly complete MB dye removal from solution [15]. The removal percentage recorded increased from 80% to 98%. The data supports that our material provides significant MB removal even at lower masses. Accordingly, the mass selected was 1.5 g/L as providing good dye removal.

3.4.2. Influence of pH on the Adsorption Behavior of Methylene Blue

Role of pH on MB dye adsorption was assessed by varying the pH of the solution from 4 to 10 by adjusting with 0.1 M HCl and 0.1 M NaOH. MB dye concentration was kept at a constant value and an adsorbant mass of 1.5 g/L (Fig.4) with a varying for a contact period of 3.5 h.

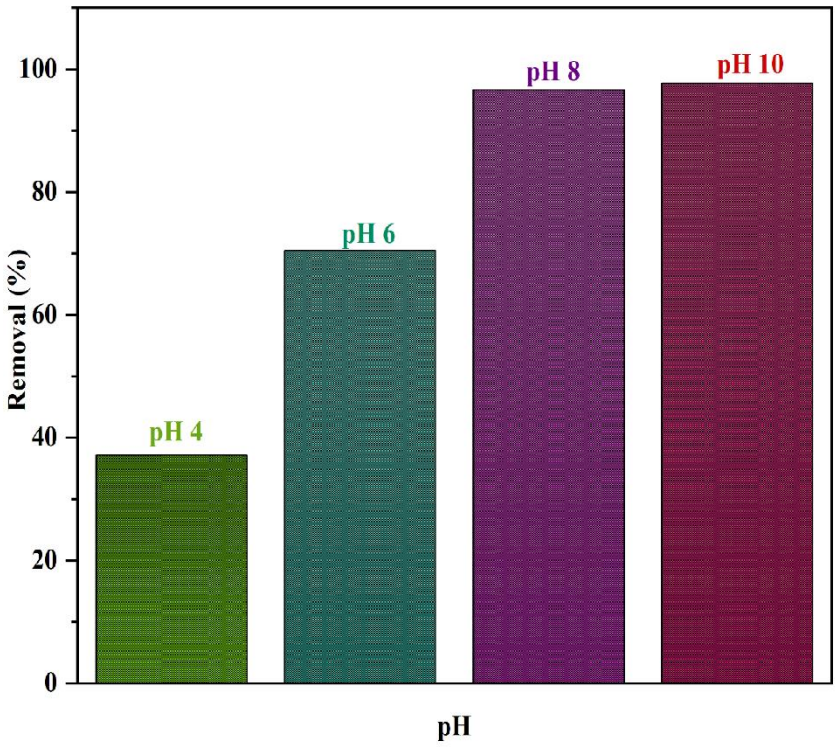

Fig. 4. Influence of pH on MB removal

Figure 4 illustrates the effect of solution pH on the removal efficiency of methylene blue (MB). The adsorption efficiency rises from 37% at pH 4 to 70% at pH 6 and reaches a maximum of 97.7% at pH 10. At acidic conditions, the adsorbent surface tends to acquire a positive charge, resulting in competition between H^+ ions and MB cations, which reduces the adsorption capacity. In contrast, under basic conditions, the surface becomes negatively charged, favoring electrostatic attraction of MB cations and thus enhancing adsorption. Consequently, the highest MB uptake is observed at higher pH values, where the balance of anions and cations in solution allows effective neutralization and binding onto the adsorbent sites [27].

3.4.3. Effect of initial concentration on Methylene MB Adsorption

The impact of the initial concentration of MB dye on the adsorption efficiency of NiO-BCHCl was explored (Fig. 5). The results in Fig.6 indicate that the % Removal decreased when the MB concentration increased. This is generally explained by the availability and sufficiency of active sites on the surface of the adsorbent to retain the pseudo-totality of dye when its concentration is low. As the primary MB concentration rises, more quickly, these active sites become saturated, thus limiting the adsorption process. This behaviour supports the principles of adsorption and highlights the importance of choosing an appropriate initial concentration when utilising MB for effective treatment [28].

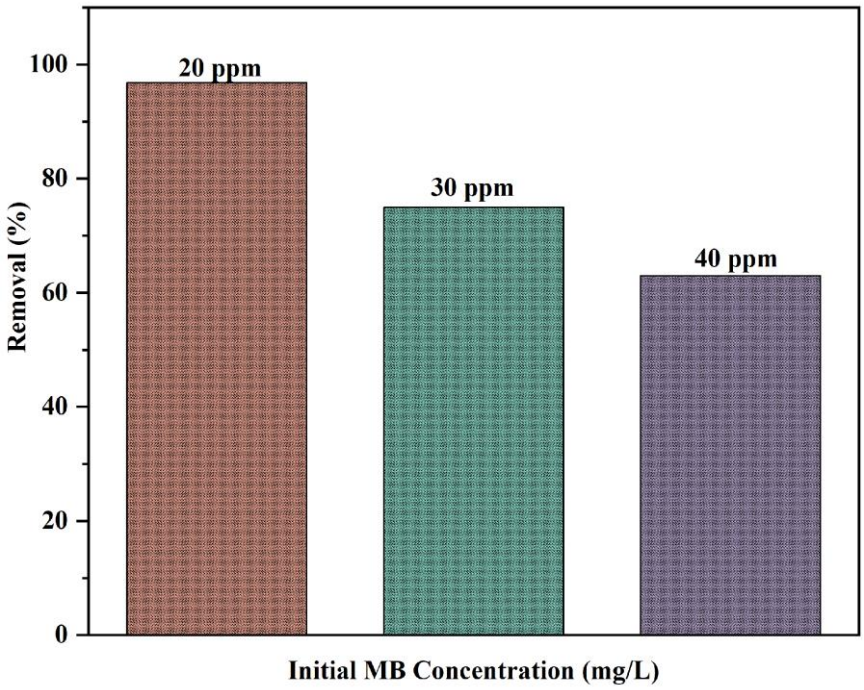

Fig. 5. Effect of Initial MB Concentration on Adsorption

3.4. Kinetic Analysis of Adsorption

By analyzing kinetic adsorption data, we understand the time aspect of adsorption reactions better, which is critical in calculating the order of the rate constant so that we can adequately design or model the adsorptio n process as kinetic parameters are important. The study of MB adsorption of NiO-BCHCl was carried out at an environmental temperature of 298 K. The experimental data collected were fit graphically to pseudofirst and pseudosecond order mathematical models of kinetics (Figure 5). Fitting of the experimental data with Nonlinear regression was employed to evaluate the models, and the SSE values are presented in Table 2.

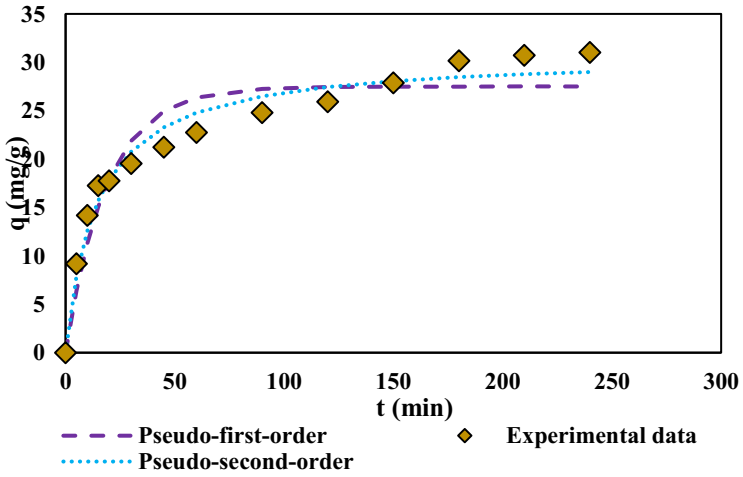

Fig. 6. Kinetic Modeling of Methylene Blue Adsorption on NiO-BCHCl

The pseudo-first-order model, with a constant K_1=0.053, shows an experimental capacity ($q_{e,exp}$) of 27,48 mg·g^{-1} and a theoretical capacity ($q_{e,th}$) of 31 mg·g^{-1}, but the high sum of squared errors (SSE = 61,69) indicates a poor fit. On the other hand, the pseudo-second-order model has a K_2=0.0023 that demonstrates a decent fit, indicating by SSE of 21,64, and it shows that only the experimental capacity ($q_{e,\,exp}$=30,73 mg·g^{-1}) is close to the theoretical value ($q_{e,\,th}$=28 mg·g^{-1}), indicating that this model describes the adsorption kinetics the best. This indicate that the adsorption process is primarily driven by chemisorption, rather than a simple physical interactions [29].

Table 2. Adsorption rate parameters for MB onto NiO-BCHCl

Approaches	Coefficients	NiO-BCHCl
Pseudo-first-order	K_1 (min^{-1})	0,05299566
	$q_{e,exp}$	27,4975579
	$q_{e,th}$	31.003
	SSE	61,6886884
Pseudo-second-order	K_2 ($g.mg^{-1}.min^{-1}$)	0,00226552
	$q_{e,exp}$	30,7271442
	$q_{e,th}$	27,9799619
	SSE	21,6415983

3.5. Study of Adsorption Isotherm Behavior

The adsorption of methylene blue (MB) on biochar was assessed, and of adsorption modeling was performed using multiple isotherms, Langmuir, Freundlich and Sips [21]. These models provide valuable information regarding the adsorption mechanism, surface properties, and interaction intensity between the adsorbent and dye. The data is shown in Fig. 7 and Table 3. Considering the data, it is reported that Sips model has the lower sum of squared errors (SSE = 19.17), the model that fits best describing MB adsorption on the composite. The model parameters of n = 0.299 and *K*s = 0.085 indicate a greater adsorption capacity and adsorption intensity therefore Sips does model a better model fit for this system. As shown in Fig. 8, the experimental adsorption data align most closely with the Sips model compared to Langmuir and Freundlich, highlighting its suitability for representing MB adsorption on NiO-BCHCl. The moderate value of the Sips constant *K*s reflects strong interactions between the adsorbent's active sites and MB molecules, while the heterogeneity factor $n_S < 1$ confirms the heterogeneous nature of the biochar surface, typical of porous materials [30].

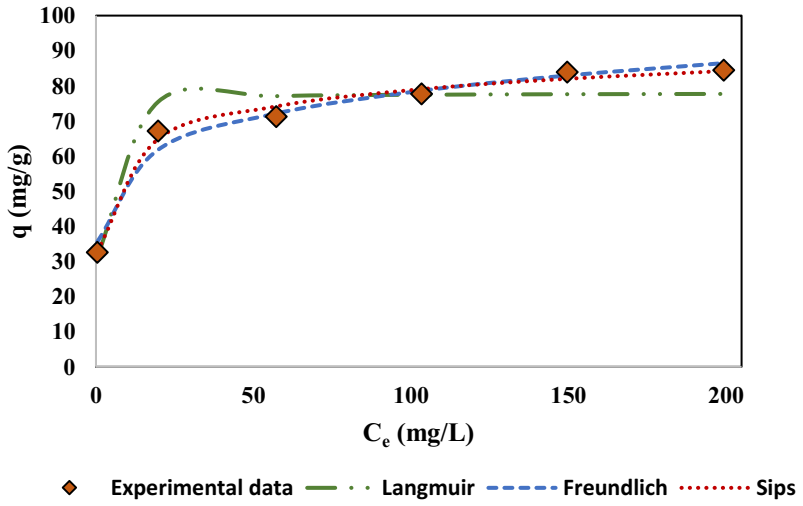

Fig. 7. Nonlinear fitting of methylene blue adsorption isotherms

Table 3. Equilibrium isotherm parameters for methylene blue adsorption onto NiO-BCHCl

Approaches	Coefficients	NiO-BCHCl
Langmuir	q_m (mg. g^{-1})	77.9582879
	K_L(L. mg^{-1})	1.5177903
	SSE	189.530168
Freundlich	n	6.88649692
	KF (mg/g) $(mg/L)^{-1/n}$	40.0809609
	SSE	44.1363932
Sips	n_S	0.29860762
	q_m (mg. g^{-1})	120.357585
	K_S (L/mg)	0.08517347
	SEE	19.1724683

3.5. Sustainability and Reusability Assessment of NiO-BCHCl Adsorbent

This regeneration study primarily aims to assess the ability of NiO-BCHCl to retain its adsorption efficiency for MB through successive adsorption cycles. The thermal regeneration behavior of NiO-BCHCl over several reuse cycles is shown in Figure .

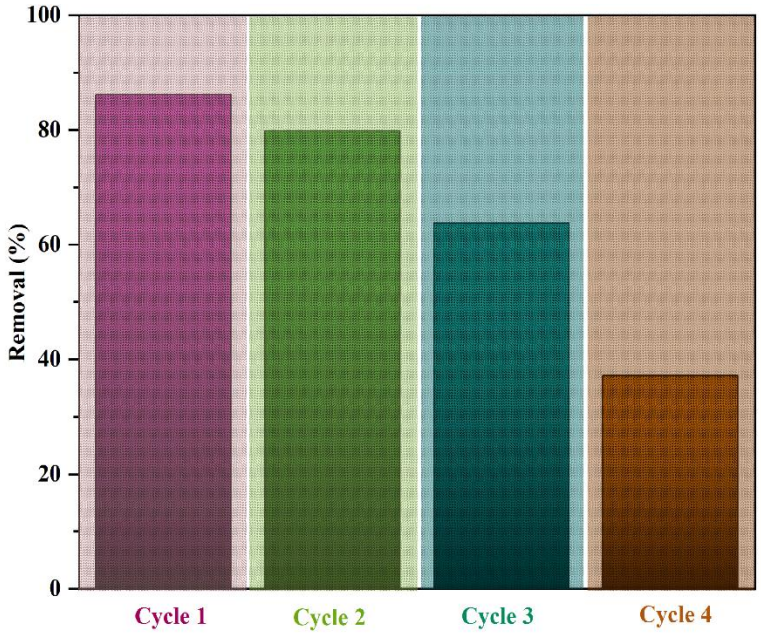

Fig. 7. Reusability and Regeneration of NiO-BCHCl

The removal performance of the NiO-BCHCl material for four consecutive adsorption-desorption (regeneration) cycles is displayed in Figure 7. The first cycle indicated a high removal performance at approximately 85–90%, revealing an effective adsorption capacity and many active sites on the material for dye adsorption. In the second cycle, the removal performance decreased slightly to approximately 75–80%, however, this indicated that there were still some active sites not lost from the first regeneration and the active surface of the adsorbent was still partially retained. A more significant decrease in performance occurred after the third cycle (approximately 60–65%), suggesting that the material was progressively saturating the more usable adsorption sites or possible minor structural changes of the material. By the fourth cycle, the removal performance had declined again substantially to approximately 35–40%, indicating that regenerated thermal loss of active sites or some loss of functional groups caused decreased adsorption and lower performance for thermal regeneration on the material. Broadly, these results show that NiO-BCHCl can be recycled, and have reasonable reusability for the first two cycles, but demonstrates clear changes in performance after multiple adsorbent regenerations.

4. Conclusion

The researcher prepared an efficient and low-cost adsorbent of MB dye from sewage sludge by pyrolysis, acid washing, and then incorporating nickel oxide. The results from BET analysis showed a significant improvement in the specific surface area of the composite to 73.62 m^2/g. In addition, the SEM/EDS analysis demonstrated successful surface modification of the Biochar and homogeneous dispersion of oxide on its surface. The synthesized composite NiO-BCHCL enhanced adsorption capability for MB pollutant. The SSE results suggest that Sips adsorption isotherm and pseudo-second order kinetic models accurately describe the adsorption process. This indicates that the adsorption process follows a chemisorption mechanism and occurs on a heterogeneous surface. These results provide an effective and economic adsorbent material to remove MB dye from contaminated water.

References

1. K. Fijalkowski, A. Rorat, A. Grobelak, and M. J. Kacprzak, Journal of Environmental Management **203**, 1126 (2017)
2. Y. Bakhtaoui, M. Ben Ali, M. Ouakki, O. El Khattabi, N. El Azzouzi, and B. Srhir, Next Materials **9**, 101072 (2025)
3. O. Ejiohuo, H. Onyeaka, A. Akinsemolu, O. F. Nwabor, K. F. Siyanbola, P. Tamasiga, and Z. T. Al-Sharify, Water Biology and Security **4**, 100341 (2025)
4. M. Gomes, T. J. Ralph, M. S. Humphries, B. P. Graves, T. Kobayashi, and D. B. Gore, Science of The Total Environment **958**, 178084 (2025)
5. M. Ben Ali, M. El Hazzat, M. Flayou, A. Moussadik, S. Belekbir, A. Sifou, M. Dahhou, M. Kacimi, A. Benzaouak, and A. El Hamidi, FirePhysChem S2667134425000239 (2025)
6. M. Ben Ali, M. Flayou, Y. Boutarba, M. El Youssfi, Y. Bakhtaoui, M. El Hazzat, A. Sifou, M. Dahhou, M. Kacimi, A. Benzaouak, and A. El Hamidi, Moroccan Journal of Chemistry **12**, 1852 (2024)
7. Y. Elkahoui, F.-Z. Abahdou, M. Ben Ali, S. Alahiane, M. Elhabacha, Y. Boutarba, and S. El Hajjaji, Reactions **6**, 23 (2025)
8. M. Ben Ali, A. Benzaouak, M. Tangarfa, Y. Abrouki, S. Belekbir, M. El. Hazzat, A. El Hamidi, and L. Abdelouahed, Case Studies in Chemical and Environmental Engineering **11**, 101219 (2025)
9. S. Khan, S. Irshad, K. Mehmood, Z. Hasnain, M. Nawaz, A. Rais, S. Gul, M. A. Wahid, A. Hashem, E. F. Abd_Allah, and D. Ibrar, Plants **13**, 166 (2024)
10. Z. Yuan, R. Nag, and E. Cummins, Science of The Total Environment **823**, 153730 (2022)
11. M. Ben Ali, A. Benzaouak, L. Valentino, A. Moussadik, M. El Hazzat, L. Abdelouahed, A. El Hamidi, and L. F. Liotta, Catalysis Today **459**, 115421 (2025)
12. S. Singh, V. Kumar, D. S. Dhanjal, S. Datta, D. Bhatia, J. Dhiman, J. Samuel, R. Prasad, and J. Singh, Journal of Cleaner Production **269**, 122259 (2020)
13. R. Sivaranjanee, P. Senthil Kumar, B. Chitra, and G. Rangasamy, Chemosphere **360**, 142382 (2024)
14. J. M. Jazić, Journal of Environmental Chemical Engineering (2024)
15. C. Zhao, B. Wang, B. K. G. Theng, P. Wu, F. Liu, S. Wang, X. Lee, M. Chen, L. Li, and X. Zhang, Science of The Total Environment **767**, 145305 (2021)
16. W. S. Gado, A. S. Morshedy, A. M. Masoud, A. E. M. E. Mohammed, E. H. Taha, A. A. El-Zahhar, M. M. Alghamdi, A. M. A. E. Naggar, and E. M. El-Fawal, RSC Adv. **15**, 13662 (2025)
17. S. Sinha, S. S. Behera, S. Das, A. Basu, R. K. Mohapatra, B. M. Murmu, N. K. Dhal, S. K. Tripathy, and P. K. Parhi, Chemical Engineering Communications **205**, 432 (2018)
18. E. D. Revellame, D. L. Fortela, W. Sharp, R. Hernandez, and M. E. Zappi, Cleaner Engineering and Technology **1**, 100032 (2020)
19. M. A. Islam, M. A. Chowdhury, Md. S. I. Mozumder, and Md. T. Uddin, ACS Omega **6**, 14481 (2021)
20. M. Vigdorowitsch, A. Pchelintsev, L. Tsygankova, and E. Tanygina, Applied Sciences **11**, 8078 (2021)
21. I. Morosanu, L. Tofan, C. Teodosiu, and C. Paduraru, Rev. Chim. **71**, 162 (2020)
22. M. Farahani, M. Kashisaz, and S. R. S. Abdullah, (n.d.)
23. Z. ALOthman, Materials **5**, 2874 (2012)
24. Q. Wen, C. Li, Z. Cai, W. Zhang, H. Gao, L. Chen, G. Zeng, X. Shu, and Y. Zhao, Bioresource Technology **102**, 942 (2011)
25. S. A. Yousif, A. H. Sulaymon, and M. M. Al-Faize, **5**, (2013)
26. R. Sadki, M. Dalimi, N. Labjar, G. A. Benabdallah, and S. E. Hajjaji, (2023)
27. E. Klimiuk, U. Filipkowska, and A. Korzeniowska, (n.d.)
28. M. A. Baghapour, B. Djahed, and M. Ranjbar, **1**, (n.d.)
29. D. Saha and H. A. Grappe, in *Activated Carbon Fiber and Textiles* (Elsevier, 2017), pp. 143–165

30. L. Lonappan, T. Rouissi, R. K. Das, S. K. Brar, A. A. Ramirez, M. Verma, R. Y. Surampalli, and J. R. Valero, Waste Management **49**, 537 (2016)